

AMS Transition Radiation Detector 4-Layer Prototype and Gas System Tests

Francesca Bucci
University of Rome "La Sapienza"

September 26 2006

The AMS Transition Radiation Detector (TRD) will provide a proton background rejection of 10^2 - 10^3 to search for SUSY dark matter signatures in the high energy cosmic rays spectrum. The TRD consists of 20 layers of straw proportional tubes interleaved with a fleece radiator material. Each tube will be filled with a Xe:CO₂ (80:20) mixture supplied by a gas system designed to operate for more than 3 years in space; the accuracy of the gas ratio is of fundamental importance for transition radiation detection. Functional tests of the gas system, together with the related electronics and control software, have been performed. In particular, studies of the mixing procedure, checks of the gas quality and tests performed on a TRD 4-layer prototype will be discussed.

1 Introduction

Alpha Magnetic Spectrometer (AMS) [1] is a high energy physics experiment that will be located on the International Space Station (ISS) to search for antimatter and dark matter in space, measuring cosmic rays spectra up to TeV scale. For these goals, AMS will use all the state of the art technologies of the modern particle physics, allowing cross checks among its subdetectors. In particular the Transition Radiation Detector (TRD), together with the Electromagnetic CALorimeter (ECAL) [2], is of fundamental importance to search for SUSY dark matter. Annihilations of neutralino, a major candidate as SUSY dark matter constituent, could produce an excess of positrons in the energy range between 10 GeV and 300 GeV; to search for neutralino annihilation signatures, we require a proton rejection factor of 10^6 . The TRD will provide a proton rejection factor of the order of 10^2 - 10^3 while the missing factor will be provided by the ECAL [3].

Transition radiation (TR) is a soft X rays emission generated when a charged particle traverses the boundary between two materials having different dielectric constants. Since the intensity of TR is proportional to the

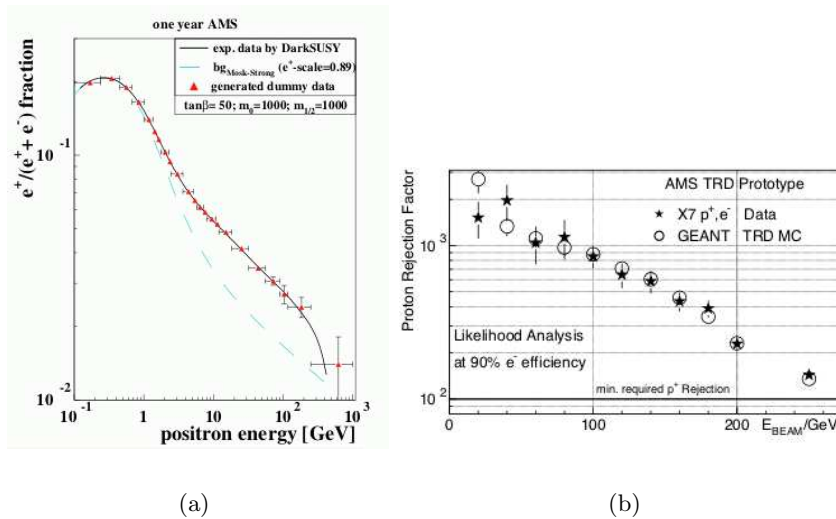


Figure 1: (a) Proton fraction expected after one year of AMS on ISS; (b) Proton rejection factor: Monte Carlo and test beam results.

Lorentz factor γ , the detection of TR allows an efficient separation of light and heavy particles. The probability of TR emission at a single surface is of the order of α so a fleece radiator is necessary to enhance this factor [4, 5, 6].

The AMS-02 TRD consists of 20 layers of straw proportional tubes, having an inner diameter of 6 mm, interleaved with 20 mm thick radiator material (polyethylene/polypropylene fibers) all placed into an octagonal support structure made of aluminium honeycomb walls covered by carbon fiber. The straw tubes are arranged into 328 modules of 16 straws each. These modules will be filled with a Xe:CO₂ (80:20) mixture used to detect the TR photons generated inside the radiator material [7, 8, 9].

The gas system designed to supply the mixture to the TRD consists of: a gas supply module (Box S) to store the amount of gas necessary for the entire duration of the mission and to provide 7 l of fresh mixture required to fill the TRD modules every day; a circulation module (Box C) to transfer the mixture from the box S to the TRD and to circulate it through the entire volume of the detector; distribution modules (Manifolds) to distribute the mixture to the TRD modules, to detect gas leaks and to isolate the leaking modules independently

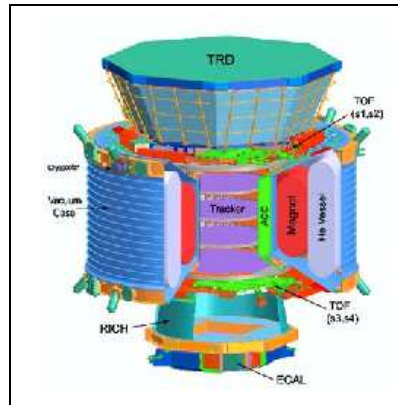


Figure 2: TRD position in AMS-02.

[10]. Each gas system module will be controlled by mean of dedicated electronic boards. The boards will be double redundant to guaranty the control of the system in case of failure of one or more electronics channels; also they will allow to operate the electromechanical divices, to chek the status of the system continously (temperature and pressure) and to shut down the system safely in case of power or communication failures [11].

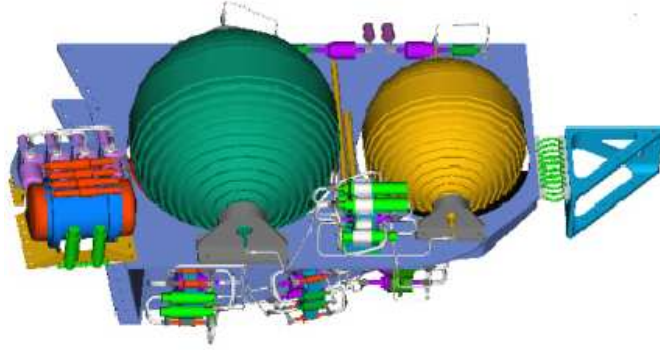


Figure 3: TRD gas system project.

2 Mixing test

The aim of the mixing test is the determination of the number of injections of Xenon and CO_2 necessary to obtain the required ratio in the mixture, as a function of gas pressure in the storage vessels. Since during the mission in space all the operations will be controlled via software, the second aim of this test is to exercise mixing cycles under computer control using the dedicated control software [12].

The mixing test has been performed using Ar instead of Xe due to the high cost of the last one. The mixture is obtained in the D vessel (see figure 4) transferring the gas from the storage bottles to the mixing vessel through box S. During the three years of mission in space, the mixture will be produced every day. Thus, taking into account the gas quantity stored, about 1000 mixing cycles will be executed before the total consumption of the reserves. For on ground verification of the mixing procedure and for a complete simulation of the processes that will take place in space, it is necessary to choose particular conditions to reproduce the whole set of operations in a limited time. For this purpose the storage bottles used in the test are filled with the same number of mol/l of gas as the flight storage vessels. For the test we used the engeneering model of the gas system in wich the gas is stored in bottles having a volume equal to 1% of the volume

of the flight storage vessels. This means that each mixing cycle executed in the test represents a 1% sample of the mixing cycles that will take place during the three years of mission. In particular, the CO₂ is stored in a volume of 150 ml with a density of 9.9 mol/l, while the Xe should be stored in a volume of 300 ml with a density of 13.4 mol/l. For this test the Xe bottle has been filled with Ar at a density of 4.3 mol/l.

The procedure to transfer the gas from the storage bottles to the mixing vessel consists of two steps: the injection of CO₂ opening valves V1b, V2b and V3b, then the injection of Ar opening valves V1a, V2a and V3a (see figure 4). Between one opening and the next one we allow to the gas enough time to expand in the buffer volumes. For each gas we performed studies of the mixing vessel pressure as a function of the opening time of the valves; this method allows to control the variation of the gas quantity transferred to the D vessel after each injection as a function of the opening times. In this way we determined the appropriate opening time for each valve; then we executed 10 mixing cycles, determining CO₂ concentration by the partial pressure method. The major difficulty in determining the mixing procedure arises from the fact that after each injection the initial conditions are changed: an accurate control of gas pressure and temperature is then necessary for every mixing cycle.

The results are shown in table 1; m corresponds to the number of Ar injections while n to those of CO₂.

The test performed shows that it is possible to determine a sequence of operations, controlled by software, that allows to obtain the desired mixture composition at each cycle.

3 Mixture quality check

The mixture quality check is made performing gain measurements using 4 proportional tubes coated with a ⁵⁵Fe source which produces 5.9 keV X rays. A MultiChannel Analyzer (MCA) allows to record the signal pulse height. For these spectra measurements we used Ar:CO₂ (80:20) premixed in a 14 l volume at a pressure of 120·10² kPa. The calibration of the multichannel analyzer was done using pulses from a pulse generator with pulse heights in the range accepted by the device (0-5 V [13]). The proper working voltage of the tubes was determined with a plateau measurement. We took measurements without high voltage applied in order to perform the pedestal subtraction.

A cut on the ADC spectrum below 60 channels was made to determine the photopeak position (see figure 5). The spectra were fitted using two gaussian functions for the photopeak and the escape peak and for the background a three parameters exponential function of the form:

$$f(x) = p_0 + p_1 \cdot \exp\left(-\frac{x}{p_2}\right).$$

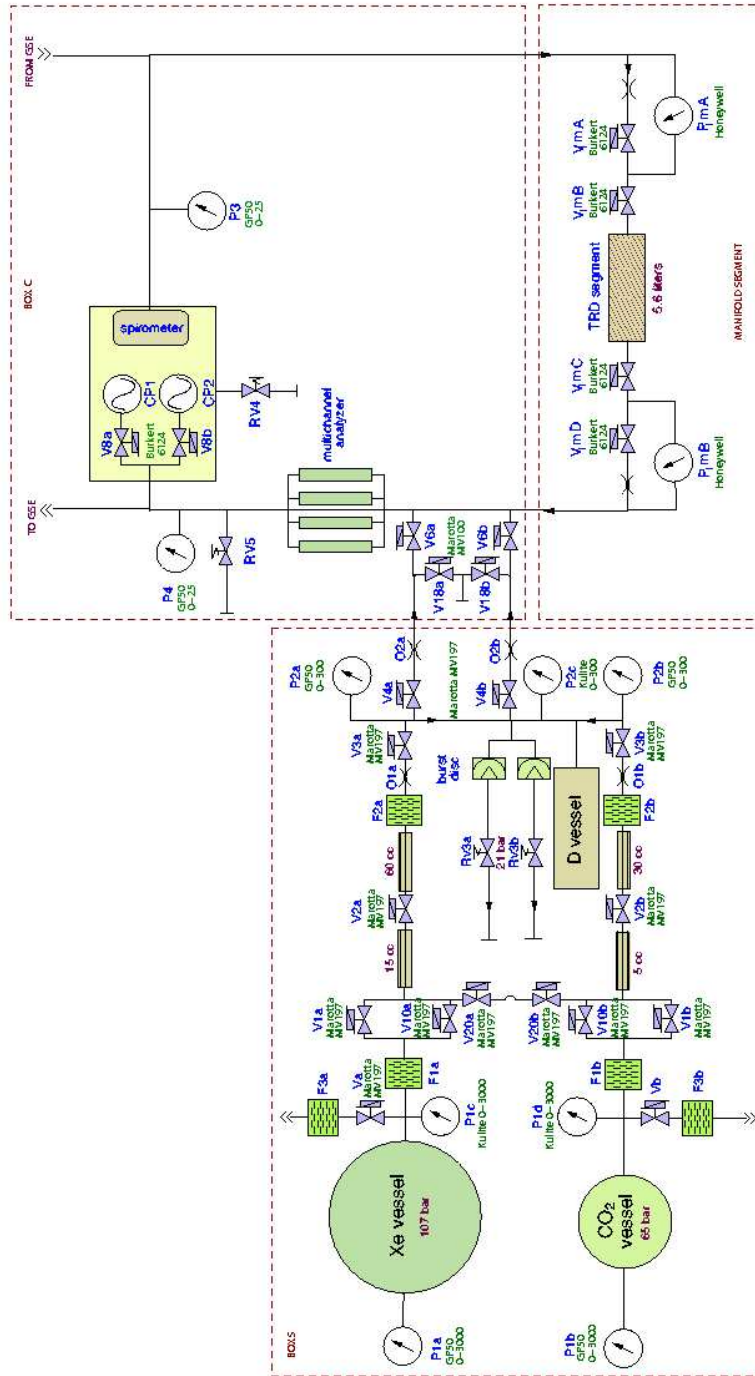


Figure 4: TRD gas system scheme

Cycle	T_i ($^{\circ}\text{C}$)	P_i^{Ar} ($\cdot 10^2$ kPa)	$P_i^{CO_2}$ ($\cdot 10$ kPa)	P_i^D (kPa)	P_f^D ($\cdot 10$ kPa)	m	n	CO_2 (%)
First	21.5 ± 0.5	136.6 ± 1.4	594.5 ± 5.9	104.2 ± 1.1	95.42 ± 0.95	4	2	19.2 ± 1.2
Second	20.6 ± 0.5	104.7 ± 1.0	579.8 ± 5.8	121.5 ± 1.2	104.56 ± 1.0	5	2	20.5 ± 1.2
Third	21.3 ± 0.5	86.29 ± 0.86	589.0 ± 5.9	112.2 ± 1.1	94.29 ± 0.94	6	2	20.0 ± 1.2
Fourth	21.3 ± 0.5	65.04 ± 0.65	587.6 ± 5.9	110.9 ± 1.1	94.47 ± 0.94	9	2	20.2 ± 1.2
Fifth	21.4 ± 0.5	43.10 ± 0.43	589.9 ± 5.9	103.5 ± 1.0	94.87 ± 0.95	10	2	19.9 ± 1.2
Sixth	22.1 ± 0.5	135.2 ± 1.4	593.2 ± 5.9	114.6 ± 1.1	100.8 ± 1.0	4	2	19.3 ± 1.2
Seventh	21.6 ± 0.5	109.9 ± 1.1	586.3 ± 5.9	109.5 ± 1.1	99.6 ± 1.0	5	2	18.1 ± 1.0
Eighth	21.2 ± 0.5	87.34 ± 0.87	581.6 ± 5.8	104.9 ± 1.0	93.13 ± 0.93	6	2	19.3 ± 1.2
Ninth	21.3 ± 0.5	66.23 ± 0.66	568.3 ± 5.7	111.4 ± 1.1	109.9 ± 1.0	8	2	20.6 ± 1.1
Tenth	21.4 ± 0.5	38.54 ± 0.38	571.1 ± 5.7	108.6 ± 1.1	90.65 ± 0.91	6	2	20.3 ± 1.2

Table 1: Initial temperature, initial pressures of Ar and CO_2 , initial and final pressure of D vessel, number of injections and CO_2 percentage for each mixing cycle.

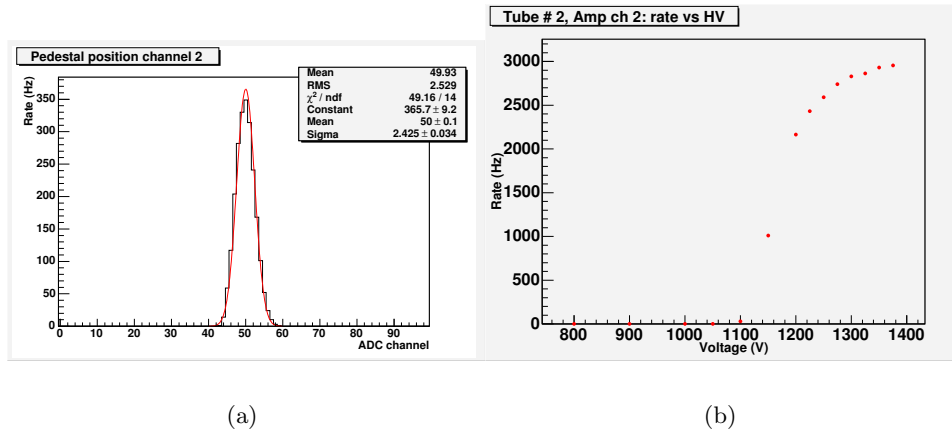


Figure 5: (a) Rate recorded by the MCA with no high voltage applied (pedestal); (b) Trend of the counting rate as a function of the high voltage.

An example of recorded spectrum is shown in figure 6. A large background, considerably increasing with the high voltage, does not allow a clear escape peak distinction. However the fit allows to identify the two expected peaks

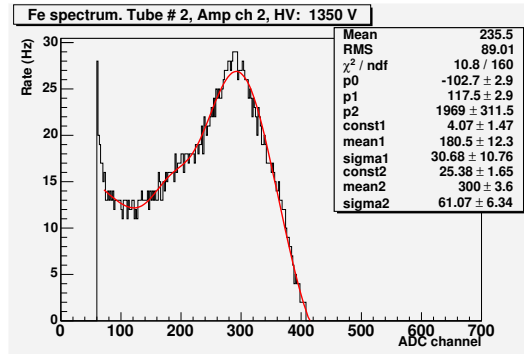


Figure 6: Spectrum generated from the ^{55}Fe source at 1350 V.

also with such a background. The peaks position as a function of the applied voltage is shown in figure 7. In ordinate the peak's ADC channel pedestal-subtracted is shown.

From the spectra analysis it is possible to obtain information about the gas density in the mixture determining gas gain from the photopeak position. This determination can be done using the Diethorn formula [14] that analytically expresses the gain G as a function of the typical values of the proportional tube geometry (tube inner radius b , anode wire radius a), of

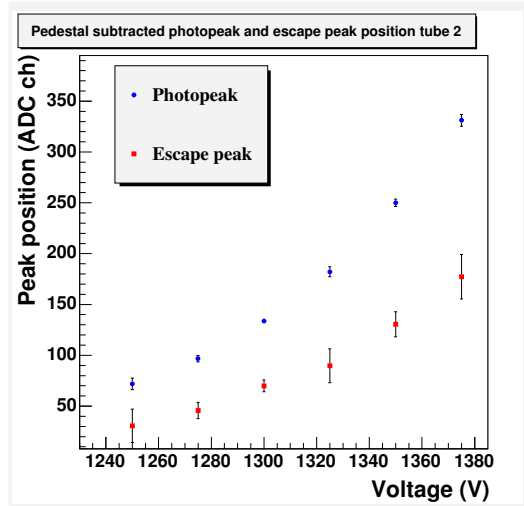


Figure 7: Photopeak and escape peak position obtained from the fit after pedestal subtraction as a function of the applied voltage.

the applied high voltage V and of the gas density ρ :

$$\ln G = \frac{\ln 2}{\ln(b/a)} \frac{V}{\Delta V} \ln \frac{V}{a \ln(b/a) E_{min}(\rho_0) (\rho/\rho_0)}. \quad (1)$$

ρ_0 represents the density at standard conditions of pressure and temperature¹ while the parameters $E_{min}(\rho_0)$ and ΔV are called Diethorn parameters and represent respectively the minimum electric field needed to start the avalanche in the ionization process and the voltage needed to ionize gas atoms.

4 Test with cosmic ray muons

The test was performed using a prototype made of 4 TRD modules, having length between 130 cm and 140 cm, interleaved with a 60 cm long, 20 mm thick radiator material placed in the middle of each module. The collected data were analyzed in order to perform track reconstruction and to study the energy deposit inside the detector. Also the energy calibration was performed recording data from the 5.9 keV photons emission of a ^{55}Fe source. The detection medium used in the test is an Ar:CO₂ (82:18) mixture. The gas was transferred from the storage bottle to the gas distribution system at $1.8 \cdot 10^2$ kPa by means of a pressure reducer, then injected into the modules at a constant flux of 0.7 l/h. The gas system consisting of the distribution system and the 4 modules is an open system where the gas is vented instead of circulating through the modules (see figure 8).

¹ $P = 101.3$ kPa, $T = 20$ °C.

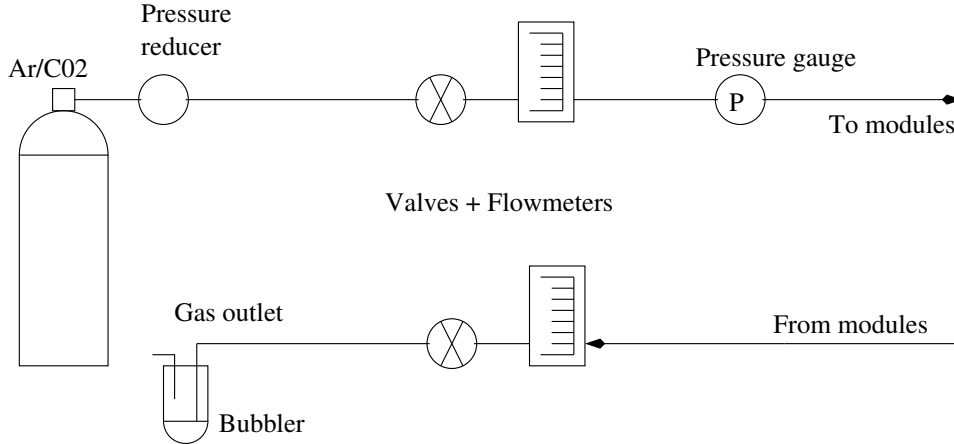


Figure 8: Scheme of the gas distribution system used in the cosmic ray muon test.

In order to study gain variations as a function of the high voltage and of the gas density, data acquisitions were made changing the high voltage applied and the gas pressure in the prototype. Temperature and pressure were checked continuously in order to determine the density. Data from each tube were corrected taking into account the pedestal position differences (see figure 9) and the unavoidable gain variations due to the mechanical precision of the modules, e.g. anode wire misalignment, then track reconstruction was performed. Only single track events with 3 or 4 hits on track and less than two hits elsewhere were selected (see figure 10); we defined a hit on track as a hit having a residual from the track linear fit smaller than 1.5 times the tube radius (3 mm).

Due to mechanical imperfections or to differences in signal preamplification from different channels of the readout electronics, the pulse height from each tube had to be corrected with respect to the mean height; to do this, we made an intercalibration defining for each channel the intercalibration factor as the ratio of the mean over the 64 channels of the most probable value (MPV) obtained from a Landau fit of the spectra, and the most probable value of the single tube spectrum, i.e. for channel i :

$$CF_i = \frac{\overline{MPV}}{MPV_i}. \quad (2)$$

In order to perform the detector intercalibration, for each readout channel the energy deposit value was multiplied by the correction value of the particular channel.

Figure 11 shows the most probable value of the energy deposited in the events recorded in an acquisition with high voltage fixed to 1400 V and gas pressure and temperature respectively of 102.84 kPa and 22.7 °C. The

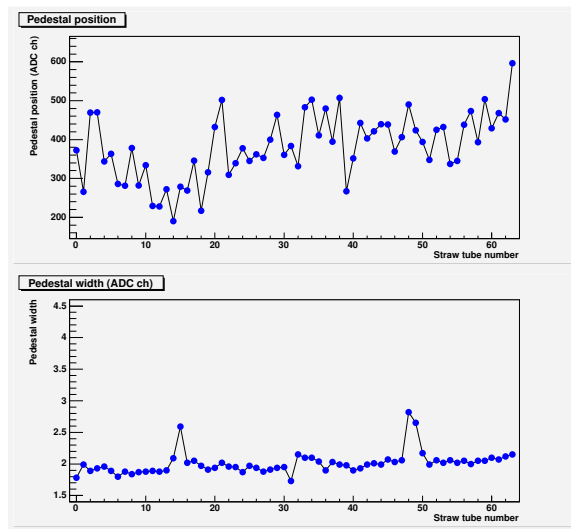
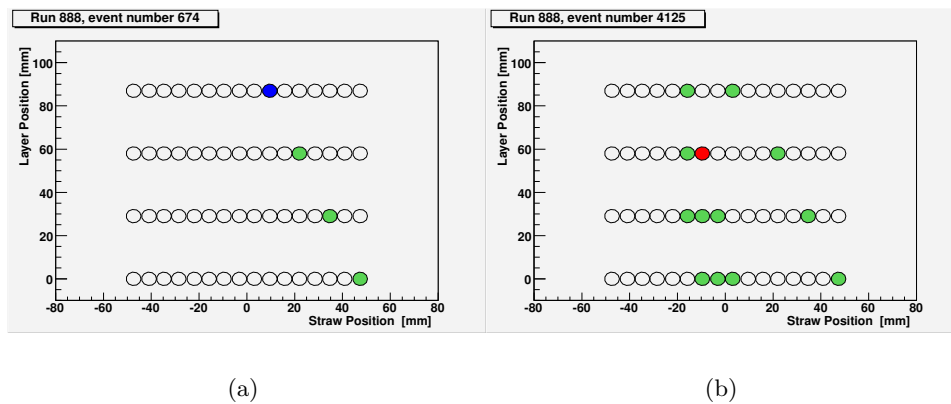


Figure 9: Pedestal position and width in terms of ADC channels.



(a)

(b)

Figure 10: (a) Example of a single track event used in the analysis; (b) Example of a rejected event.

histogram includes the pulse height of all the hits on track recorded in the single track events; the pulse height in the histogram takes into account pedestal subtraction and intercalibration corrections.

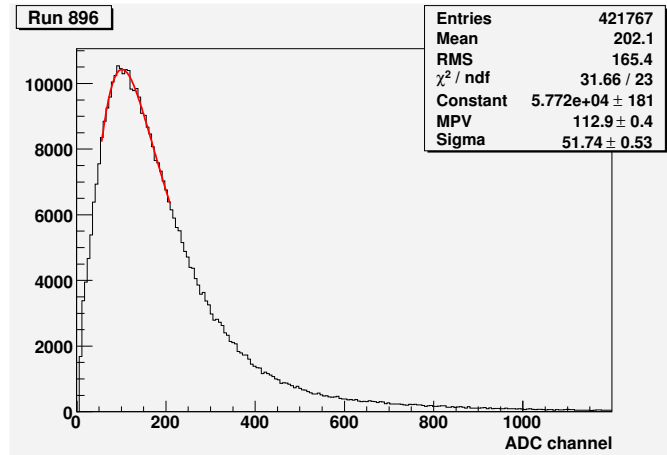


Figure 11: Spectrum recorded in the TRD modules at a high voltage of 1400 V and a pressure of $1028.4 \cdot 10^2$ Pa at 22.7 °C.

The energy calibration of the detector was made recording the emission spectra of a ^{55}Fe source. In these measurements we used a random trigger. The spectra do not show a clear photopeak but a continuous distribution up to a knee corresponding to the nominal energy of the photon emitted; this shape is due to the unavoidable cosmic contribution to the spectrum registered using a random trigger. An example of such a spectrum is shown in figure 12.

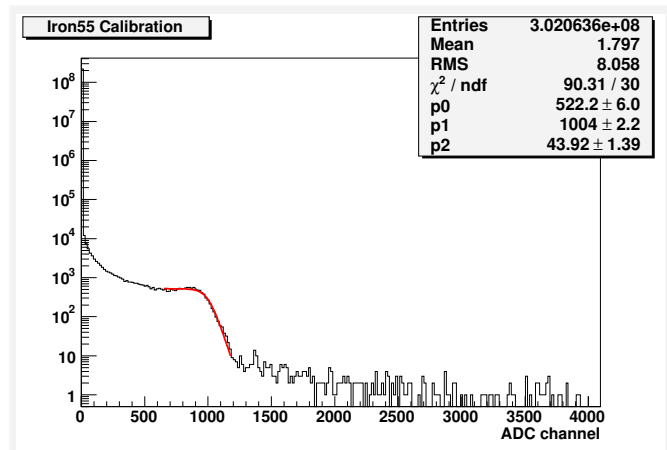


Figure 12: Spectrum recorded for the detector energy calibration using a ^{55}Fe source.

In this case the energy calibration factor was obtained performing a fit on the distribution knee using a three parameters Fermi function of the form

$$f(x) = \frac{A}{\exp(\frac{x-B}{C}) + 1}. \quad (3)$$

It can be shown that the parameter σ of the gaussian fit usually done to obtain the photopeak position is correlated to the parameter C of the Fermi function [15]; it is then possible to get the photopeak position performing a Fermi fit on the spectra.

Neglecting the gas density variations due to pressure and temperature variations, the relation between the ADC channel number and the energy of the photon emitted by the ^{55}Fe source is:

$$(996.3 \pm 2.1)\text{ADC Channel} \equiv 5.9 \text{ keV} \quad (4)$$

from which we get an energy calibration factor (ECF) given by:

$$\text{ECF} = (5.92 \pm 0.01) \frac{\text{eV}}{\text{ADC Channel}} \quad (5)$$

The above energy calibration factor was applied to the data related to the spectrum shown in figure 11 leading to the result shown in figure 13; the fit result shows that the most probable value of the energy deposited inside the detector is $(669.6 \pm 2.3 \text{ eV})$ to be compared with the expected value for MIPs crossing a mean Ar:CO₂ (82:18) thickness of 3 mm at the same pressure and temperature, i.e. approximately a value of 806.2 eV [16, 17].

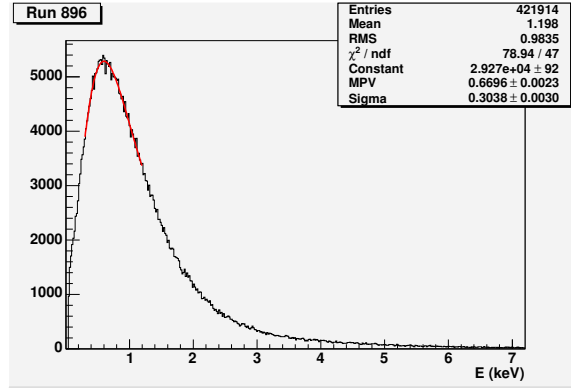


Figure 13: Energy deposited in the 4 TRD modules at a high voltage of 1400 V, a pressure of $1028.4 \cdot 10^2 \text{ Pa}$ at $22.7 \text{ }^\circ\text{C}$.

5 Conclusions

From the energy deposit it is possible to deduce the dependence of the gas gain on the gas density. The relative gas gain variation $\frac{G}{G_0}$ (equivalent to $\frac{MPV}{MPV_0}$), at fixed applied high voltage of 1350 V, was plotted as a function of the appropriate gas density normalized to the standard density² $\rho_0 \simeq 1.69 \text{ gl}^{-1}$ (see figure 14).

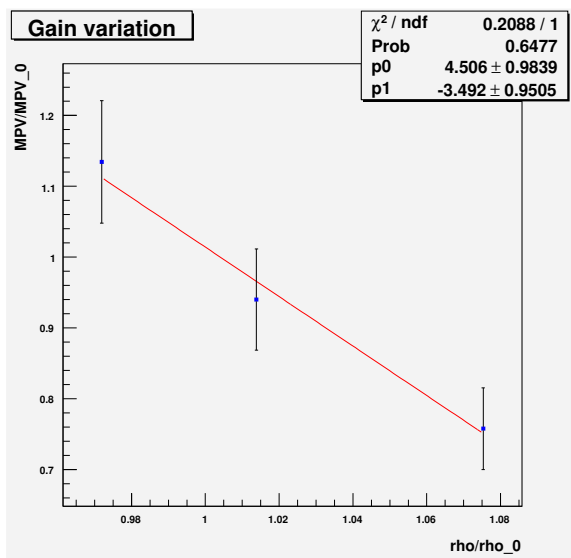


Figure 14: Relative gas gain as a function of the relative gas density.

According to the slope derived from the linear fit, a 1% variation in the gas density leads to a gain variation of $(3.49 \pm 0.95)\%$, to be compared with an expected gain variation of the order of 5%.

Acknowledgments

I would like to thank Prof. Bruno Borgia, Dr. Francesca Spada and the whole AMS-TRD group of the university of Rome “La Sapienza” and INFN for giving me the chance to contribute to this interesting work and for their help. Furthermore very special thanks goes to Prof. Ulrich Becker (MIT, Boston) and Dr. Thorsten Siedenbueg (RWTH, Aachen) for their kind support and guide and for the useful and so instructive discussions.

²Density of the Ar:CO₂ (82:18) mixture at standard conditions of temperature and pressure.

References

- [1] B. Borgia. *The Alpha Magnetic Spectrometer on the International Space Station*. *IEEE Transactions on Nuclear Science*, 52(6):2786–2792, 2005.
- [2] F. Cadoux et al. *The AMS-02 Electromagnetic Calorimeter*. *Nuclear Physics B Proceedings Supplements*, 113:159–165, 2002.
- [3] S. Gentile. *The Performance of the Transition Radiation Detector of the AMS-02 experiment*. In *Proc. of IEEE Nuclear Science Symposium, Portland, Oregon, USA*, 2003.
- [4] B. Dolgoshein. *Transition radiation detectors*. *Nuclear Instruments and Methods in Physics Research*, A326:434–469, 1993.
- [5] V. L. Ginzburg and V. N. Tsytovich. *Transition radiation and transition scattering*. Adam Hilger, 1990.
- [6] X. Artru, G. B. Yodh, and G. Mennessier. *Practical theory of multilayered transition radiation detector*. *Physical Review D*, 12(5), September 1975.
- [7] F. Hauler. *The AMS-02 TRD for the International Space Station*. In *Proc. of IEEE Nuclear Science Symposium, Portland, Oregon, USA*, 2003.
- [8] J. Olzem. *Construction of the AMS-02 Transition Radiation Detector for the International Space Station*. In *Proc. of 29th International Cosmic Ray Conference Pune*, 2005.
- [9] T. Kirn and T. Siedenburg. *The AMS-02 Transition Radiation Detector*. *Nuclear Instruments and Methods in Physics Research*, A535:165–170, 2004.
- [10] U. Becker, J. Burger, and P. Fisher. *TRD gas system summary and specifications*, April 4 2003.
- [11] A. Bartoloni, B. Borgia, F. Bucci, and F.R. Spada. *AMS-02 TRD Gas Slow Control System Specification v 4.1*. INFN Sezione Roma I, 2006.
- [12] F. Bucci, S. Gentile, A. Lebedev, and F.R. Spada. *WINCAN v. 2.2 A Linux-based Slow Control interface for the AMS TRD Gas System*. Università di Roma “La Sapienza” e INFN, LNS MIT Cambridge (USA).
- [13] *MCA 8000A Specifications*. www.amptek.com/mca8000a.html.
- [14] W. Blum and L. Rolandi. *Particle identification with drift chambers*. Springer-Verlag, 1993.

- [15] T. Kirn, November 30 2000. AMS-02 TRD Meeting, Boston.
- [16] *Atomic and Nuclear Properties of Materials*. <http://pdg.lbl.gov/AtomicNuclearProperties>.
- [17] *NIST Chemistry WebBook*. <http://webbook.nist.gov/chemistry/form-ser.html>.